


ORIGINAL ARTICLE

SGLT-1-specific inhibition ameliorates renal failure and alters the gut microbial community in mice with adenine-induced renal failure

Hsin-Jung Ho^{1,2} | Koichi Kikuchi^{2,3} | Daiki Oikawa⁴ | Shun Watanabe^{2,5} | Yoshitomi Kanemitsu⁶ | Daisuke Saigusa⁷ | Ryota Kujirai⁸ | Wakako Ikeda-Ohtsubo⁹ | Mariko Ichijo² | Yukako Akiyama² | Yuichi Aoki⁷ | Eikan Mishima² | Yoshiaki Ogata⁵ | Yoshitsugu Oikawa¹⁰ | Tetsuro Matsushashi¹⁰ | Takafumi Toyohara^{1,2} | Chitose Suzuki² | Takehiro Suzuki^{1,2} | Nariyasu Mano⁶ | Yoshiteru Kagawa¹¹ | Yuji Owada¹¹ | Takane Katayama¹² | Toru Nakayama⁴ | Yoshihisa Tomioka¹² | Takaaki Abe^{1,2,5} 

¹Department of Medical Science, Tohoku University Graduate School of Biomedical Engineering, Sendai, Japan

²Division of Nephrology, Endocrinology and Vascular Medicine, Tohoku University Graduate School of Medicine, Sendai, Japan

³Department of Medical Megabank, Tohoku University, Sendai, Japan

⁴Department of Biomolecular Engineering Applied Life Chemistry, Tohoku University Graduate School of Engineering, Sendai, Japan

⁵Department of Clinical Biology and Hormonal Regulation, Tohoku University Graduate School of Medicine, Sendai, Japan

⁶Department of Pharmaceutical Sciences, Tohoku University Hospital, Sendai, Japan

⁷Department of Integrative Genomics, Tohoku Medical Megabank Organization, Tohoku University, Sendai, Japan

⁸Laboratory of Oncology, Pharmacy Practice and Sciences, Tohoku University Graduate School of Pharmaceutical Sciences, Sendai, Japan

⁹Laboratory of Animal Products Chemistry, Graduate School of Agricultural Science, Tohoku University, Sendai, Japan

¹⁰Department of Pediatrics, Tohoku University Graduate School of Medicine, Sendai, Japan

¹¹Department of Organ Anatomy, Tohoku University Graduate School of Medicine, Sendai, Japan

¹²Laboratory of Molecular Biology of Bioresponse, Graduate School of Biostudies, Kyoto University, Kyoto, Japan

Correspondence

Takaaki Abe, Department of Medical Science, Tohoku University Graduate School of Biomedical Engineering, Sendai, Japan.

Email: takaabe@med.tohoku.ac.jp

Funding information

This work was supported in part by a National Grant-in-Aid for Scientific Research from the Ministry of Education, Culture, Sports, Science, and Technology of Japan (18H02822, 20K20604, 21H02932),

Abstract

Sodium-dependent glucose cotransporters (SGLTs) have attracted considerable attention as new targets for type 2 diabetes mellitus. In the kidney, SGLT2 is the major glucose uptake transporter in the proximal tubules, and inhibition of SGLT2 in the proximal tubules shows renoprotective effects. On the other hand, SGLT1 plays a role in glucose absorption from the gastrointestinal tract, and the relationship between SGLT1 inhibition in the gut and renal function remains unclear. Here, we examined the effect of SGL5213, a novel and potent intestinal SGLT1 inhibitor, in a renal failure (RF) model. SGL5213 improved renal function and

Hsin-Jung Ho, Koichi Kikuchi, Daiki Oikawa, and Shun Watanabe contributed equally to this work.

This is an open access article under the terms of the Creative Commons Attribution License, which permits use, distribution and reproduction in any medium, provided the original work is properly cited.

© 2021 The Authors. *Physiological Reports* published by Wiley Periodicals LLC on behalf of The Physiological Society and the American Physiological Society.

and the Japan Agency for Medical Research and Development (AMED) 20ek0210133h0001, 20ak0101127h0001, and J21000294 and Taisho Pharmaceutical Co.

reduced gut-derived uremic toxins (phenyl sulfate and trimethylamine-*N*-oxide) in an adenine-induced RF model. Histological analysis revealed that SGL5213 ameliorated renal fibrosis and inflammation. SGL5213 also reduced gut inflammation and fibrosis in the ileum, which is a primary target of SGL5213. Examination of the gut microbiota community revealed that the Firmicutes/Bacteroidetes ratio, which suggests gut dysbiosis, was increased in RF and SGL5213 rebalanced the ratio by increasing Bacteroidetes and reducing Firmicutes. At the genus level, *Allobaculum* (a major component of Erysipelotrichaceae) was significantly increased in the RF group, and this increase was canceled by SGL5213. We also measured the effect of SGL5213 on bacterial phenol-producing enzymes that catalyze tyrosine into phenol, following the reduction of phenyl sulfate, which is a novel marker and a therapeutic target for diabetic kidney disease DKD. We found that the enzyme inhibition was less potent, suggesting that the change in the microbial community and the reduction of uremic toxins may be related to the renoprotective effect of SGL5213. Because SGL5213 is a low-absorbable SGLT1 inhibitor, these data suggest that the gastrointestinal inhibition of SGLT1 is also a target for chronic kidney diseases.

KEYWORDS

chronic kidney disease, gut microbiota, phenyl sulfate, sodium glucose cotransporter 1 (SGLT1), uremic toxins

1 | INTRODUCTION

Chronic kidney disease (CKD) is a worldwide health problem, and its complications increase the risk of progression to end-stage renal disease (ESRD), cardiovascular disease, and all-cause mortality (Jha et al., 2013; Weiner et al., 2004). Diabetic kidney disease (DKD) occurs in approximately 20–30% of all diabetic patients and is a major cause of ESRD, cardiovascular events, and death (Ritz & Orth, 1999). Recently, sodium-dependent glucose cotransporters (SGLTs) have attracted considerable attention as new targets for type 2 diabetes (T2DM) (Alicic et al., 2019). In the kidney, SGLT2 is responsible for reabsorption of more than 90% of filtered glucose, and SGLT1 reabsorbs the remaining 10% (Kalra et al., 2016; Wright et al., 2011). Several SGLT2 inhibitors have been approved for the treatment of T2DM, and it has been reported that the SGLT2-specific inhibitors empagliflozin (Wanner et al., 2016) and canagliflozin (Perkovic et al., 2018) are associated with slower progression of kidney disease, suggesting a possible renoprotective effect in T2DM.

In contrast, SGLT1 plays an important role in glucose absorption in the small intestine (Wright et al., 2011). Intestinal SGLT1 mRNA expression and glucose uptake are increased in patients with T2DM (Kuroda et al., 2019). Therefore, SGLT1 inhibitors are an attractive option for the treatment of T2DM (Kuroda et al., 2019). In addition,

recent studies have revealed that inhibition of SGLT1 in the small intestine results in reduced glucose uptake and that unabsorbed glucose transiently reaches the lower small intestine (Oguma et al., 2015; Roder et al., 2014), which led to the conjecture that the glucose load may alter the gut microbiota composition and reduce gut-derived uremic toxins. Indeed, we previously reported that the dual sodium/glucose co-transporter (SGLT) 1/2 inhibitor canagliflozin reduced the accumulation of gut-derived uremic toxins, indoxyl sulfate (IS), and *p*-cresyl sulfate (PCS), by altering the intestinal environment in an adenine-induced renal failure (RF) mouse model (Mishima et al., 2018). However, the precise relationship between SGLT1-specific inhibition and renal function as well as gut-derived uremic toxins is still unclear. Here, we examined the effect of a low-absorbable SGLT1 inhibitor, SGL5213 (Io et al., 2019; Kuroda et al., 2019), on renal function, uremic toxins, and gut microbiota in an adenine-induced RF model.

2 | MATERIALS AND METHODS

2.1 | Materials

SGL5213, a low-absorbed SGLT1 inhibitor (Io et al., 2019; Kuroda et al., 2019) was supplied by Taisho Pharmaceutical Co., Ltd. Adenine was purchased from

Wako Pure Chemical Industries, and a sterilized adenine-containing diet (0.2%) was purchased from CLEA Japan. S-(*o*-nitrophenyl)-L-cysteine (SOPC) was synthesized according to the method described by Phillips et al. (1989), in which 2-nitrofluorobenzene was replaced with 1,2-dinitrobenzene.

2.2 | Animal model

All experiments were approved in accordance with the guidelines of the Animal Ethics Committee of Tohoku University School of Medicine. C57BL/6N mice were purchased from CLEA Japan Inc. Seven-week old mice were used for the intestinal glucose transit experiment, as well as for the 2 week administration of SGL5213 in the normal and adenine-induced RF models.

For the experiment of intestinal glucose experiment, normal (Nor), and adenine-induced RF mice were administered a 10 mg/kg glucose with or without bolus of 100 mg/kg SGL5213 or vehicle (dH₂O) in a 100 μ l volume after 20–22 h of fasting.

After 1 h, the mice were sacrificed, and blood, urine, feces, and tissues were collected.

To generate the RF model, the mice were fed a CE-2 diet containing 0.2% adenine (0.2% adenine diet) for at least 6 weeks (Mishima et al., 2015). After that, the 0.2% adenine diet was subsequently fed for an additional week and then changed to the normal diet for another week, as previously reported (Kamijo-Ikemori et al., 2016). During these 2 weeks, the mice were orally administered 10 mg/kg SGL5213 (dissolved in water) twice per day. Water intake and food intake were estimated by calculating the total water intake in one group cage (divided per mouse number). At the end of the study, the mice were sacrificed after isoflurane anesthesia, and blood, urine, feces, kidney, intestine, cecum, and colon tissues were collected. Blood urea nitrogen and biochemical parameters were assessed using a blood analyzer (i-STAT; Fuso Pharmaceutical Industries). The plasma, urine, feces, and intestinal glucose levels of the control and RF mice were measured using LabAssay™ Glucose (Mutarotase-GOD method, Wako) according to the manufacturer's instructions. Mouse tail blood pressure was measured as we previously described (Nanto-Hara et al., 2020).

2.3 | Histological analysis

Tissues were fixed in 10% neutral-buffered formalin and embedded in paraffin. Kidney sections were stained with hematoxylin and eosin (H&E) and Masson's

trichrome (MT) staining (Mishima et al., 2015; Nanto-Hara et al., 2020). The renal tubular areas in the cortex were quantitatively analyzed using MT-stained sections using Image J analysis software (National Institutes of Health). Two pathologists, who were blinded to the treatment of the individual mice, performed the evaluation.

2.4 | Quantitative polymerase chain reaction

Tissue samples were homogenized in TRIzol reagent (Invitrogen, Thermo Fisher Scientific), and mRNA was extracted according to the manufacturer's instructions. cDNA synthesis was performed using a Transcriptor First Strand cDNA Synthesis Kit (Roche). Primers were purchased from Applied Bio systems/Thermo Fisher Scientific (Table S1).

2.5 | Measurement of uremic toxins

Plasma concentrations of TMAO, phenyl sulfate (PS), and IS were measured using liquid chromatography–tandem mass spectrometry (LC-MS/MS), as described previously (Kanemitsu et al., 2017). Briefly, chromatographic separation was performed on a Nanospace SI-2 LC system (Shiseido) using a Scherzo SS-C18 analytical column (50 \times 2.0 mm i.d., 3.0 μ m, Imtakt). A guard column (2 \times 5 mm, 3 μ m) was used to protect the analytical column containing the same material as the analytical column, which was fitted between the analytical column and the autosampler. The column effluent was monitored using a TSQ Ultra triple quadrupole mass spectrometer (Thermo Fisher Scientific) equipped with a heated electrospray ionization source system. Samples were analyzed in the single reaction monitoring mode using the ion transitions: m/z 76.05 \rightarrow 58.10 for TMAO, m/z 172.99 \rightarrow 93.30 for PS, and m/z 212.03 \rightarrow 131.95 for IS. Deuterated internal standards were used for all analytes.

2.6 | Microbiome analysis

Genomic DNA of gut microbiota was extracted from the murine fecal contents, and 16S rRNA genes in the DNA samples were analyzed using a MiSeq sequencer (Illumina) as described previously (Murakami et al., 2015) by Bioengineering Lab. Co. Ltd.. Briefly, microbial genomic DNA was extracted using a phenol-chloroform standard protocol with vigorous shaking with 0.1-mm

zirconia/silica beads. The V1-V2 region of the 16S rRNA gene was amplified from the isolated DNA using the bacterial universal primer set 27Fmod (5'-ACACTCTTTCCC TACACGACGCTCTTCCGATCTAGRGTGTTGATYMTGG CTCAG-3') and 338R (5'-GTGACTGGAGTTCAGACGTG TGCTCTTCCGATCTTGCTGCCTCCCGTAGGAGT-3'). MiSeq sequencing was performed according to the manufacturer's instructions. The 16s rRNA reads were analyzed using QIIME (v1.9.1) (Caporaso et al., 2010). Microbiome data were deposited in the DDBJ database (Accession # DRA011963).

2.7 | TPL enzyme activity

The TPL enzyme of *Erwinia herbicola* was purified as previously reported (Katayama et al., 2000). Enzyme activity was measured with 0.6 mM SOPC (Watkins & Phillips, 2001) in 50 mM potassium phosphate, pH 8.0, at 25°C, following the decrease in absorbance at 370 nm ($\epsilon = -1.86 \times 10^3 \text{ M}^{-1} \text{ cm}^{-1}$) (Phillips, 1987). The inhibitory effects of 2-Aza tyrosine (Kikuchi et al., 2019; Watkins & Phillips, 2001) and SGL5213 on TPL were determined using SOPC as the substrate, as described above. The reaction mixtures contained 50 mM triethanolamine hydrochloride, pH 6.8–8.8, or 50 mM Bis-tris propane hydrochloride, pH 8.3–9.4, 2.5 mM dithiothreitol, 50 μM PLP, 0.2 mM NADH, 2 units of LDH, and L-tyrosine, and the reaction was initiated by the addition of TPL (Sundararaju et al., 1997).

2.8 | Statistical analysis

Results are presented as mean \pm SE. The data of the Chao 1 and Shannon index are presented as box plots. To compare two groups, we used Student-*t* test. Comparisons in three group were assessed using a Dunnett's test with JMP Pro software version 13 (SAS Institute Inc.). Statistical significance was set at a *p* value <0.05.

3 | RESULTS

3.1 | Effects of the SGLT1-selective inhibitor SGL5213 in normal and RF mice

To examine the effect of SGL5213 on the acute postprandial peak glucose concentration, we administered a bolus of SGL5213 and examined the glucose dynamics in normal and RF mice (Figure 1a). In normal mice, the plasma glucose level was reduced by SGL5213; in the small intestine, SGL5213 increased the intestinal fluid and the unabsorbed amount of intestinal glucose, resulting in an increase in the total amount of intestinal glucose (Figure 1b). Under RF conditions, SGL5213 also reduced blood glucose levels and increased both intestinal fluid and total intestinal glucose levels (Figure 1c). These results suggest that SGL5213 inhibits intestinal glucose uptake during RF.

3.2 | Effect of SGL5213 on adenine-induced RF mice

Next, we examined the effect of long-term administration of SGL5213 in the RF model (Table 1, Figure 1d). Body weight and food intake were reduced, and water intake was increased in the adenine groups (Figure 1e). After changing to the normal diet for another week, body weight, and food intake increased. In the RF-SGL5213 group, water intake was reduced, and Hb and Hct were increased compared with the RF group, suggesting an improvement in renal function (Table 1). We also measured heart rate and blood pressure in normal, RF, and RF + SGL5213 mice, but there were no significant differences in heart rate, systolic blood pressure, and mean blood pressure. Only diastolic blood pressure in RF mice was lower than that in normal mice but we did not observe any significant meaning in it. This suggests that the renoprotective effect of SGL5213 was not dependent on blood pressure (Figure S1).

FIGURE 1 Experimental design and effect of SGL5213 on gut fluid and glucose of normal and renal failure mice. (a) Mice were divided into four subgroups: (1) a control group (*Control*), (2) an SGL5213 (100 mg/kg)-bolus treated control group (SGL5213), (3) an adenine-induced renal failure group (*RF*), and (4) an SGL5213 (100 mg/kg)-bolus treated RF group (*RF + S*). Mice were administered a 10 mg/kg glucose with or without bolus of 100 mg/kg SGL5213 or vehicle (dH₂O) in a 100 μl volume after 20–22 h of fasting. (b) Plasma glucose, intestinal fluid, and intestinal total glucose in normal mice. Control: normal group ($n = 8$); SGL5213: Normal diet treated with SGL5213 (100 mg/kg/day) group ($n = 8$ –9 each). Statistical analyses were performed using a Student-*t* test. * $p < 0.05$, *** $p < 0.01$, and **** $p < 0.001$ were treated as statistically significant. (c) Plasma glucose, intestinal fluid, and intestinal total glucose in renal failure mice. RF: renal failure group ($n = 8$); RF + S: RF treated with SGL5213 (100 mg/kg/day) group ($n = 8$ –9 each). Data were mean \pm SEM. Data were mean \pm SEM. Statistical analyses were performed using a Student-*t* test. * $p < 0.05$, *** $p < 0.01$, and **** $p < 0.001$ were treated as statistically significant. (d) Mice were divided into three subgroups: (1) a control normal diet group (*Control*), (2) an adenine-induced uremic renal failure group (*RF*), and (3) an SGL5213 (10 mg/kg/day)-treated RF group (*RF + S*). (e) Body weight was measured weekly. Food and water intake were measured every other day

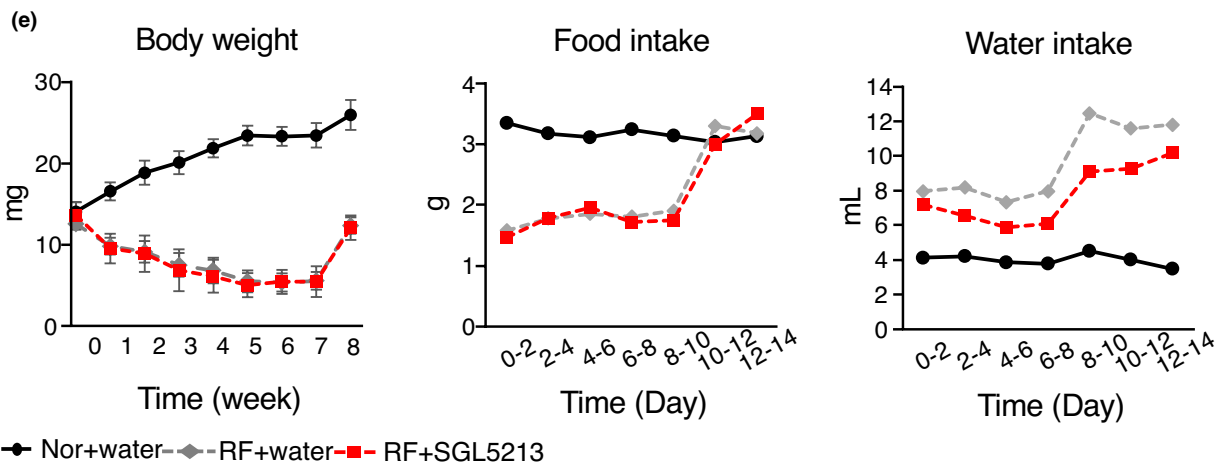
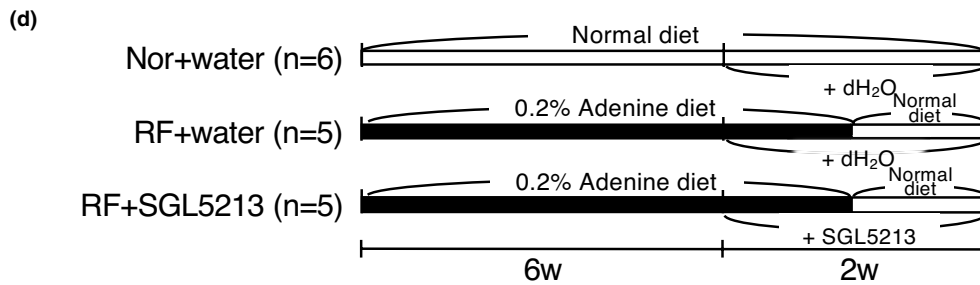
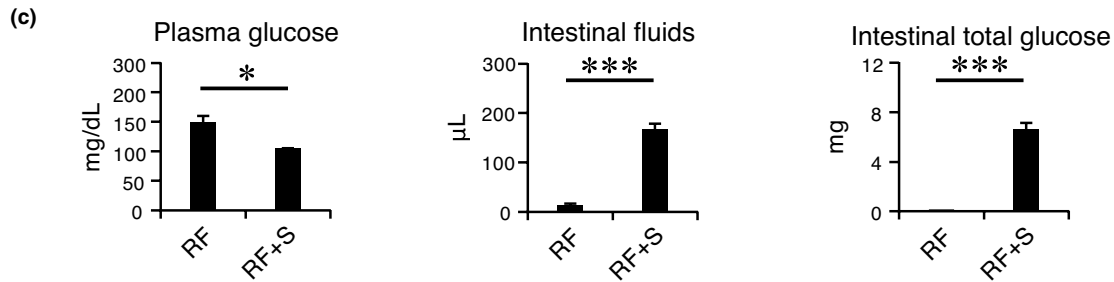
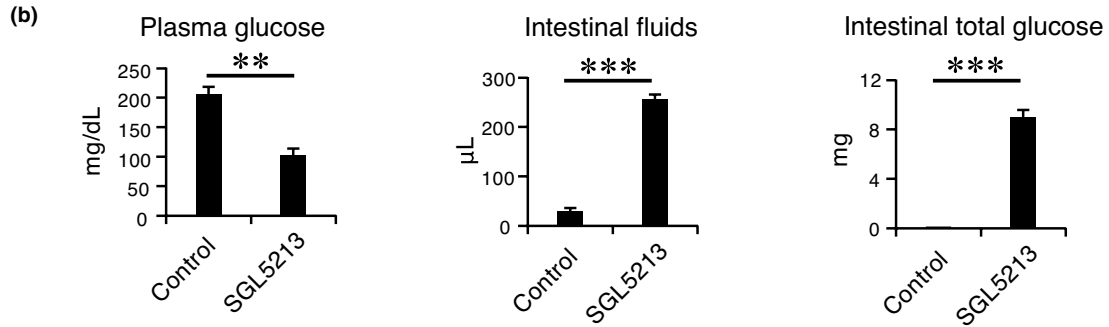
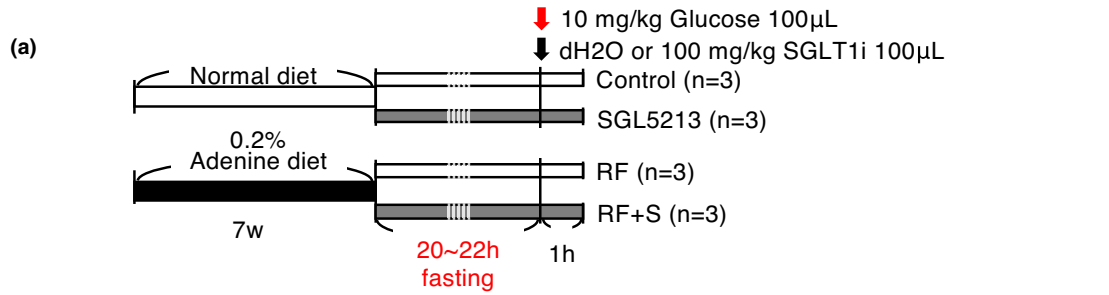


TABLE 1 Water and food intake, plasma glucose levels, and biochemical parameters in adenine-induced renal failure model

	Control (n = 6)	RF (n = 5)	RF + S (n = 5)
Na (mmol/L)	147.5 ± 0.8	145.4 ± 1.1	145.6 ± 0.5
K (mmol/L)	5.2 ± 0.2	5.1 ± 0.3	5.2 ± 0.3
Cl (mmol/L)	109.7 ± 0.4	108.6 ± 0.9	108.8 ± 1.0
tCO ₂ (mmol/L)	23.0 ± 0.5	23.4 ± 0.9	23.6 ± 0.2
Hb (mg/dL)	15.7 ± 0.2***	10.2 ± 0.2	11.2 ± 0.3*
Hct (%PCV)	46.2 ± 0.7***	30.0 ± 0.6	33.0 ± 0.8*
AnGap (%PCV)	21.0 ± 0.6	19.2 ± 0.9	19.0 ± 0.8

Note: Body weight, food intake, water intake, and biochemical parameters (Na, K, Cl, tCO₂, total carbon dioxide; Ht, hematocrit; and Hb, hemoglobin) were measured. Statistical analysis was performed using a Dunnett's test compared with the RF group. **p* < 0.05 and ****p* < 0.01 were treated as statistically significant. RF; renal failure, RF + S; and renal failure + SGL5213 (10 mg/kg).

Mean ± SEM, *n* = 5–6, **p* < 0.05, ****p* < 0.001 versus RF (Dunnett test).

Next, we performed biochemical analyses of metabolites. Blood and urine glucose levels were not altered by SGL5213 treatment. 1,5-anhydroglucitol (1,5-AG), a non-metabolizable glucose analog that competes with glucose for renal reabsorption (Balis et al., 2014), was reduced (Figure 2a). Although the bioavailability of SGL5213 was only 0.17% (Kuroda et al., 2018), it suggests that SGL5213 inhibits kidney SGLT1 to some extent without affecting serum or the total amount of urinary glucose.

We also measured fecal glucose and found that there was no significant difference between the levels of the RF and RF + SGL5213 groups (Figure 1), suggesting that utilization of excreted glucose in the intestine by gut microbiota and consumption caused a low level of fecal glucose in the RF + SGL5213 group.

Next, we examined renal function and the metabolite analysis (Figure 2b). In the adenine-induced RF mice, BUN and Cr levels were increased. Under these conditions, the increased BUN and Cr levels in RF mice were significantly reduced by SGL5213.

Metabolomic analysis revealed that ureic acid was significantly and allantoin was tend to be reduced by SGL5213, further suggesting the improvement of renal function and oxidative stress, as allantoin is a major xanthine product in mice as well as a marker of oxidative stress (Kand'ar & Zakova, 2008). No change of the cholesterol level was seen in this experiment.

In RF, the serum values of citrate, fumarate, oxalate, and malate were significantly increased, so that the sum of the concentrations of the TCA cycle intermediates was increased (Biasioli et al., 1987). Therefore, we measured the levels of the TCA components. As shown in Figure 2c, the serum levels of citrate, isocitrate, α -ketoglutarate, fumarate, and malate were increased in the RF group, and

SGL5213 significantly reduced the aconitic acid, citrate, α -ketoglutarate, fumarate, and malate levels, further suggesting an improvement in renal function (data also in Figure S2). Because SGL5213 exhibited low membrane permeability and the bioavailability of SGL5213 was very low in vivo, indicating a low absorbability (Kuroda et al., 2019), the main active site of SGL5213 is suggested to be in the gut.

Recently, we reported that canagliflozin, a dual SGLT1/2 inhibitor, reduced the plasma levels of gut-derived uremic toxins, IS, and *p*-cresyl sulfate (PCS), by influencing the intestinal environment in mice with adenine-induced RF (Mishima et al., 2015). Therefore, we examined the effect of SGL5213 on gut-derived uremic toxin levels. As shown in Figure 2d, the plasma levels of IS, PS, and TMAO were significantly increased in the RF mice, and the elevated plasma levels of TMAO and PS were significantly reduced in SGL5213 mice, although the elevated level of IS did not change. As we reported, IS, PS, and PCS were 100% gut-derived. Concerning TMAO, 70% of TMAO was gut derived, and 30% was from TMA in a chaw with fish meal. Therefore, the changes in PS and TMAO were very close to the changes in the gut microbial community (Kikuchi et al., 2019; Mishima, Fukuda, Mukawa, et al., 2017). These results suggest that SGL5213 alters the specific gut microbial community during RF.

Next, we performed histological analysis of the kidney. The cortical tubular area described by MT staining was decreased in the RF group, and the reduction was significantly recovered by SGL5213 (Figure 3a, left). In addition, the increase in the renal fibrotic area in the RF group was ameliorated by SGL5213. Immunostaining with F4/80 (an antigen that is a macrophage-restricted cell surface glycoprotein) showed an increase in the fibrotic area in the RF mice, and this increase was reduced by SGL5213.

Quantitative analysis also showed that reduction of fibrotic area (Figure 3a, right panel). These data suggest the recovery of the tissue damaged by SGL5213.

Next, we examined fibrosis- and inflammation-related gene levels by qPCR. The expression levels of fibrosis-related genes, *acta2* (α -SMA), *col1a1* (collagen I), and *tgfb1* (TGF β 1), were upregulated in the RF mice, and the upregulated levels of *acta2* and *tgfb1* were significantly decreased by SGL5213 (Figure 3b). The expression levels of inflammation-related genes, *emr1* (F4/80), *ccl2* (MCP-1), and *cd68* (CD68) were increased in RF, and the upregulated levels of *ccl2* and *cd68* were significantly decreased by the drug. These data suggest that SGL5213 ameliorated renal damage and reduced fibrosis and macrophage infiltration in an adenine-induced RF model.

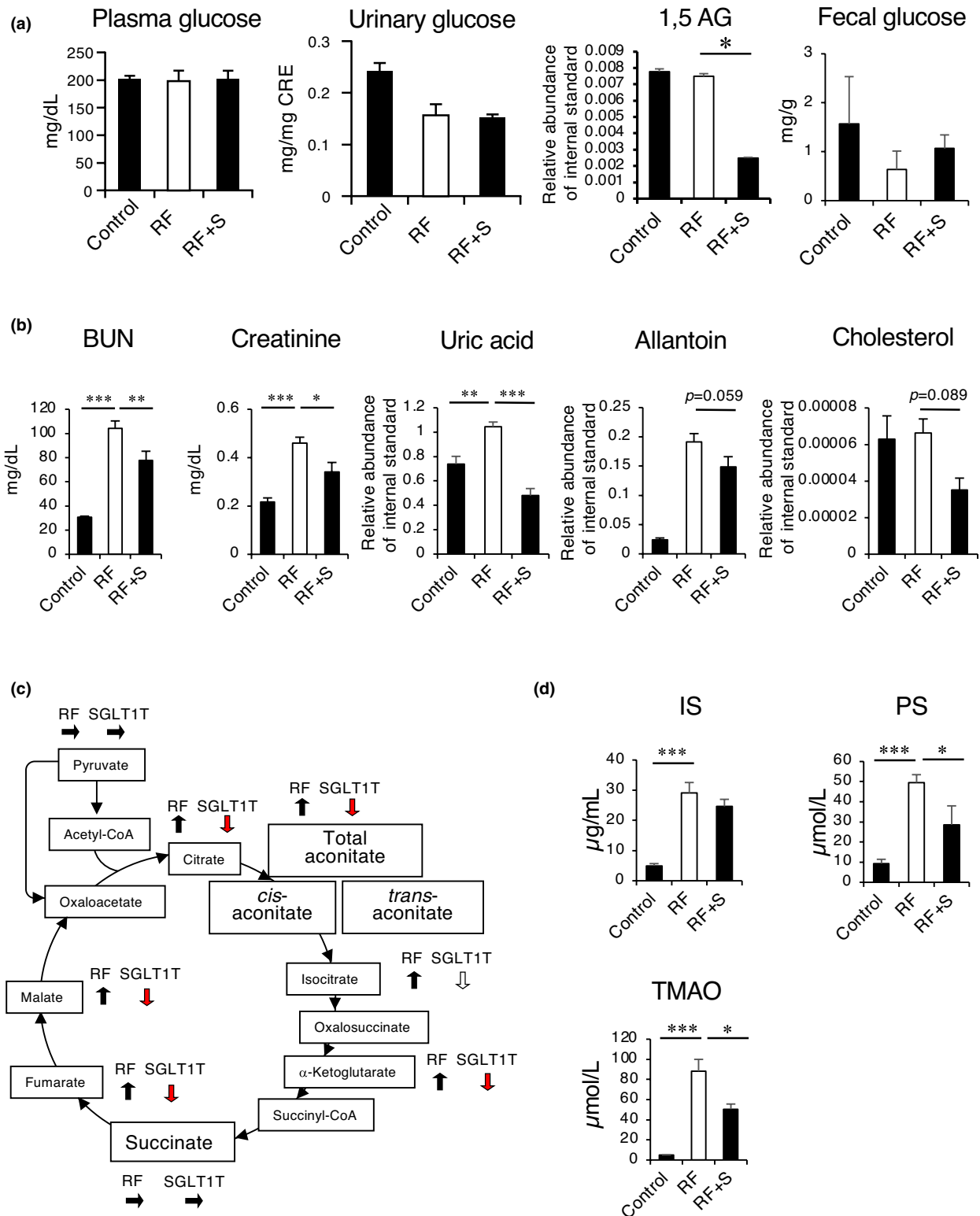


FIGURE 2 SGL5213 improved renal function in an adenine-induced renal failure model. (a) Plasma glucose, urine glucose, and 1,5-AG levels in adenine-induced renal failure model. (b) The plasma BUN, Cr, Urea, allantoin, and cholesterol levels in adenine-induced renal failure model mice treated with SGL5213 (10 mg/kg/day) for 14 days. Cont: control group ($n = 8$); RF; renal failure group ($n = 6$); RF treated with SGL5213 (10 mg/kg/day) group ($n = 8-9$ each). (c) The plasma TCA component levels. (d) The plasma level of IS, PS, and TMAO in the adenine-induced renal failure model. Cont; control group ($n = 8$), RF: renal failure group ($n = 6$), RF treated with SGL5213 (10 mg/kg/day) group ($n = 8-9$ each). Data were mean \pm SEM. Statistical analysis was performed using a Dunnett's test. * $p < 0.05$ and *** $p < 0.01$ were treated as statistically significant

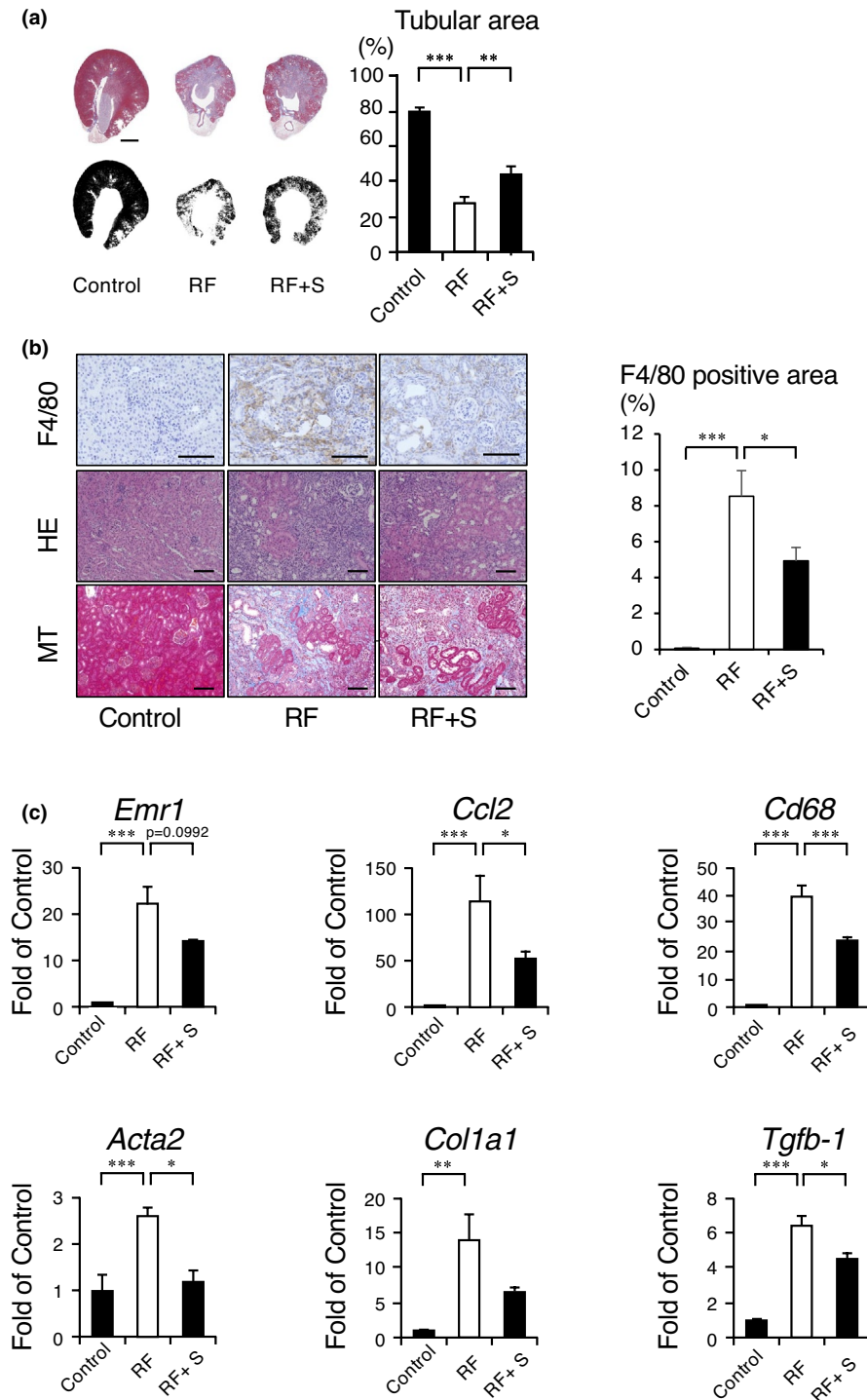


FIGURE 3 Histological examination of the adenine-induced renal failure mouse kidney. (a) Masson's trichrome (MT) staining was performed. Morphometric analysis of the cortical tubular area was calculated based on the images. Bars = 500 μ m. Data were mean \pm SEM. Statistical analysis was performed using a Dunnett's test. * $p < 0.05$ and *** $p < 0.01$ were treated as statistically significant. (b) Representative histological images of the adenine-induced renal failure mouse kidney. Masson's trichrome stained (MTS) and immunohistochemical analysis of F4/80 was also performed. Bars = 50 μ m. Arrow indicates the F4/80-positive macrophages. (c) Quantitative analysis of fibrotic and inflammatory genes. The mRNA levels of *emr1*, *ccl2*, *cd68*, *act2*, *col1a1*, and *tgf-1* were measured by real-time PCR. The mRNA expression levels were normalized with β -actin. Data were mean \pm SEM. Statistical analysis was performed using a Dunnett's test. * $p < 0.05$ and *** $p < 0.01$ were treated as statistically significant

3.3 | SGL5213 reduced gut inflammation and fibrosis

It has been reported that disruption of the tight junction in the gastric, ileal, jejunal, and colonic epithelium was observed in RF (Nanto-Hara et al., 2020; Vaziri et al., 2013). This impairment of barrier function in CKD could contribute to the pathogenesis of systemic inflammation in CKD (Vaziri et al., 2016). We then examined the effect of SGL5213 on the uremic gut in an adenine-induced RF

model. MT staining showed fibrotic changes in the RF group, but the fibrotic areas were decreased by SGL5213 (Figure 4a). Immunostaining with F4/80 also showed an increase in the area of the RF, and this increase was recovered by SGL5213. qPCR analysis revealed that the expression levels of fibrotic genes *acta2* and *col1a1* were significantly increased, but the expression level of *tgfb1* was not increased in the RF group (Figure 4b). The upregulated expression levels of *acta2* and *col1a1* were significantly reduced by SGL5213. In addition, qPCR analysis of

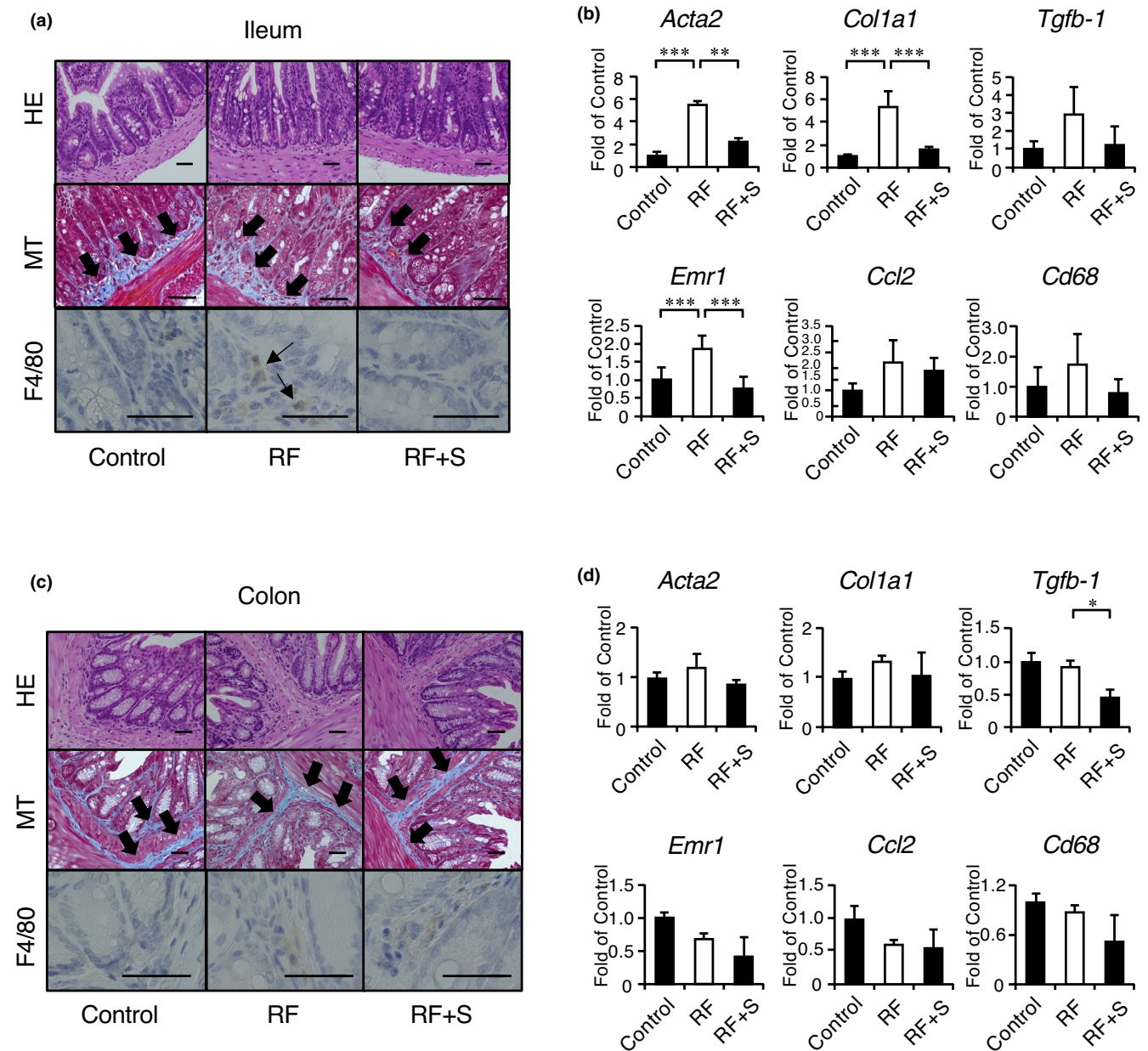


FIGURE 4 SGL5213 ameliorated intestinal fibrosis and inflammation in the adenine-induced renal failure model. (a) Representative histological images of the adenine-induced renal failure mouse ileum. Masson's trichrome (MT) staining was performed. In the MT, the arrow indicates the fibrotic area. In the MTS, the arrow indicates dense eosinophilic granules. Bars = 50 μ m. Immunohistochemical analysis of F4/80 was also performed. Arrow indicates the F4/80-positive macrophages. (b) Quantitative analysis of fibrotic and inflammatory genes in the ileum. The mRNA levels of fibrotic genes (*act2*, *col1*, and *tgfb1*) and inflammatory genes (*emr1*, *ccl2*, and *cd68*) were measured by real-time PCR. The mRNA expression levels were normalized to that of GAPDH. Data were mean \pm SEM. Statistical analyses were performed using a Dunnett's test. * $p < 0.05$ and *** $p < 0.01$ were treated as statistically significant. (c) Representative histological images of adenine-induced renal failure in the mouse colon. SR staining was performed. Bars = 50 μ m. Immunohistochemical analysis of F4/80 and claudin 1 was also performed. (d) Quantitative analysis of fibrotic and inflammatory genes in the colon. The mRNA levels of fibrotic genes (*act2*, *col1*, and *tgfb1*) and inflammatory genes (*emr1*, *ccl2*, and *cd68*) were measured by real-time PCR. The mRNA expression levels were normalized to that of GAPDH. Data were mean \pm SEM. Statistical analyses were performed using a Dunnett's test. * $p < 0.05$ and *** $p < 0.01$ were treated as statistically significant

the inflammatory genes *emr1*, *ccl2*, and *cd68* also revealed that the gene expression level of F4/80 (*emr1*) was significantly increased in the RF group, and this increase was significantly reduced by SGL5213 treatment (Figure 4b).

These data suggest that SGL5213 reduces ileal fibrosis, accompanied by RF.

In contrast, in the colon, neither MT nor F4/80 staining showed significant changes in the RF and RF + SGL5213

groups compared with the control group (Figure 4c). qPCR analysis also revealed that the expression levels of *acta2*, *colla1*, and *tgfb1* were not changed in the RF groups, and the expression level of *tgfb1* was only decreased in the RF + SGL5213 group compared to the RF group. Furthermore, no significant changes were observed in the inflammatory genes *emr1*, *ccl2*, and *cd68* (Figure 4d). These results suggest that SGL5213 reduces gut inflammation and fibrosis mainly in the ileum following modification of the gut environment.

3.4 | SGL5213 altered gut-derived uremic toxins and the gut microbiota community in RF mice

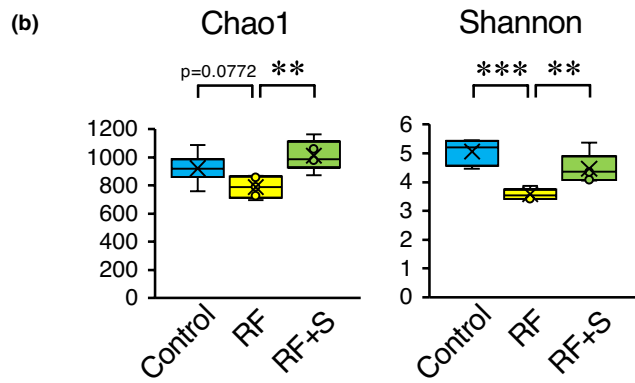
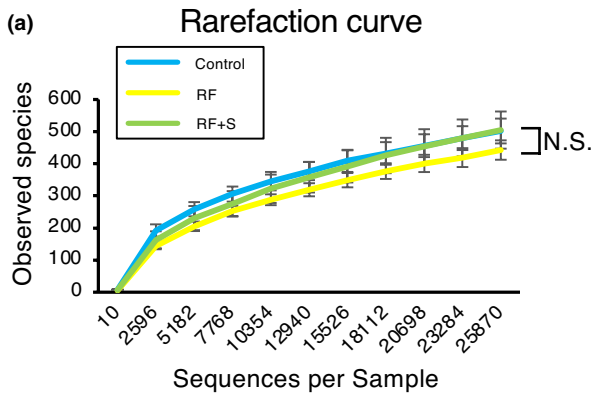
To elucidate the effect of SGL5213 on the gut microbial community, we performed fecal 16S rRNA gene analysis. As shown in Figure 5a, the rarefaction curve showed no differences in species richness among the groups. However, the Chao 1 index (richness) and Shannon index evenness revealed lower richness and diversity in the RF group, and the reduced Chao 1 and Shannon indices were restored by SGL5213 (Figure 5b). In addition, UniFrac analysis (unweighted, left panel and weighted, right panel) revealed that the clustering patterns of normal, RF, and SGL5213 groups were separated (Figure 5c). These data suggest that SGL5213 affects the gut microbial community during RF.

Next, we focused on the parts of the microbiome in which the abundances were positively correlated with the plasma gut-derived uremic toxin levels in RF and were changed by SGL5213. Figure 5d shows the microbial population at the phylum, class, order, family, and genus levels. At the phylum level, we found three major populations: Firmicutes, Bacteroidetes, and Actinobacteria. The Firmicutes/Bacteroidetes (F/B) ratio has been widely considered a signature of gut dysbiosis (Yang et al., 2015). As shown in Figure 5e, compared with control mice, the RF mice showed an increased F/B ratio caused by the expansion of Firmicutes and contraction of Bacteroidetes.

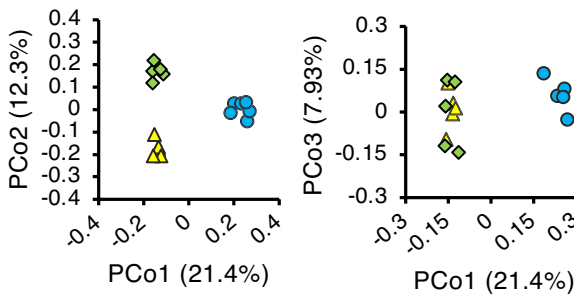
In addition to the reduced gut-derived uremic toxins, SGL5213 was able to rebalance the dysbiotic gut microbiota by reducing the F/B ratio by increasing Bacteroidetes but reducing the OTU (operational taxonomic unit) level of Firmicutes. Furthermore, Actinobacteria was increased in the RF group, and this increase was significantly attenuated by SGL5213. These results further suggest that SGL5213 alters the specific gut microbial community during RF.

Figure 6 shows the changes in the gut microbial community throughout the bacterial tree diagram. Among these, we next focused on the parts of the microbiome in which the abundance positively correlated with the plasma uremic toxin levels when modified by SGL5213. At the genus level within Firmicutes, the most represented genera in all subjects were *Allobaculum* (a major component of Erysipelotrichaceae). *Allobaculum* was significantly increased in the RF group, but this increase was significantly ameliorated by SGL5213. In contrast, *Turicibacter*, another component of Erysipelotrichaceae, was increased in the RF and further increased in the SGL5213 group. These data suggest that the genus component of Erysipelotrichaceae is related to RF and that SGL5213 affects the composition. Within Bacteroidetes, *Bacteroides* and *S24-7:g* (major components of Bacteroidetes), and *Rikenellaceae (unclassified)* were decreased in the RF group, and the reduction was canceled by SGL5213. The increase in Firmicutes genera and decrease in Bacteroidetes mainly changed the F/B ratio in RF, and SGL5213 altered the composition following the reduction of uremic toxins in the RF mice (Figure 3e). In addition, *Bifidobacterium*, a member of the family Bifidobacteriaceae, was significantly increased in the RF group, but the increase was canceled by SGL5213. In contrast, *Corynebacterium* was only increased in the RF + SGL5213 group. Taken together, these data suggest that SGL5213 altered the gut microbiota community in mice with adenine-induced RF, which may be responsible for the reduction in gut-derived uremic toxins. The detailed data of taxa at the rank of order, family, and genus are also arranged in Figures S1–S5.

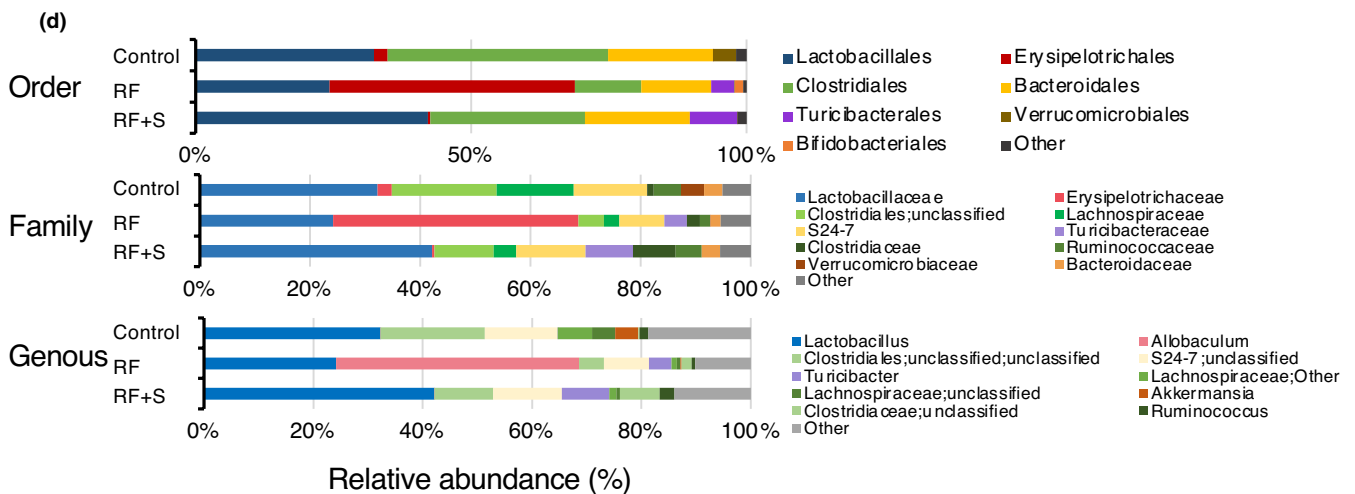
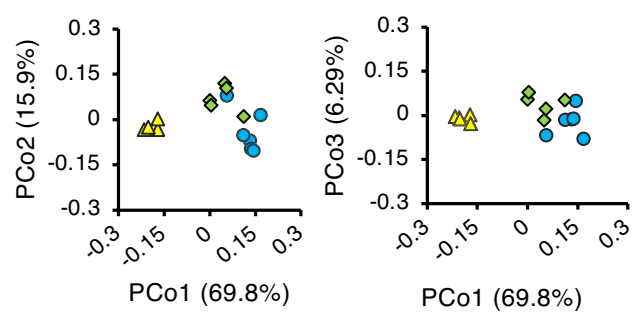
FIGURE 5 Effect of SGL5213 on the gut-derived uremic toxins and microbiome community in renal failure mice. (a) Observed OTU rarefaction analysis. OTU rarefaction curves of gut microbiota were used to estimate richness in the control (Cont), renal failure (RF), and RF + SGL5213 groups (10 mg/kg/day). (b) OTU-based α -diversity of each microbiome. Significant diversity was seen between control versus RF and RF versus RF + SGL5213 by Chao 1 (left) and Shannon (right) analyses. (c) Principal coordinates analysis of the microbiome profiles using weighted UniFrac. The scores for the first principal component (PC1) versus the second principal component (PC2) and PC1 versus the third principal component (PC3) are presented. (d) Relative abundance of microbiota based on the average abundance of each subgroup at order, family, and genus levels. Major subgroups are indicated on the right. Genera displaying a significant change among the three groups. The y-axis indicates the abundance of each microbe (%). Control ($n = 8$), RF ($n = 6$), RF + SGL5213 ($n = 8$), and RF + SGL5213 ($n = 9$) in each group. Data were mean \pm SEM. (e) The Firmicutes/Bacteroidetes ratio (F/B ratio) was calculated as a biomarker of gut dysbiosis. A decrease of Bacteroidetes along with an increase of Firmicutes resulted in a dysbiosis signature of gut microbiota in the renal failure. SGL5213 significantly rebalanced the F/B ratio. Statistical analyses were performed using a Dunnett's test. * $p < 0.05$ was treated as statistically significant



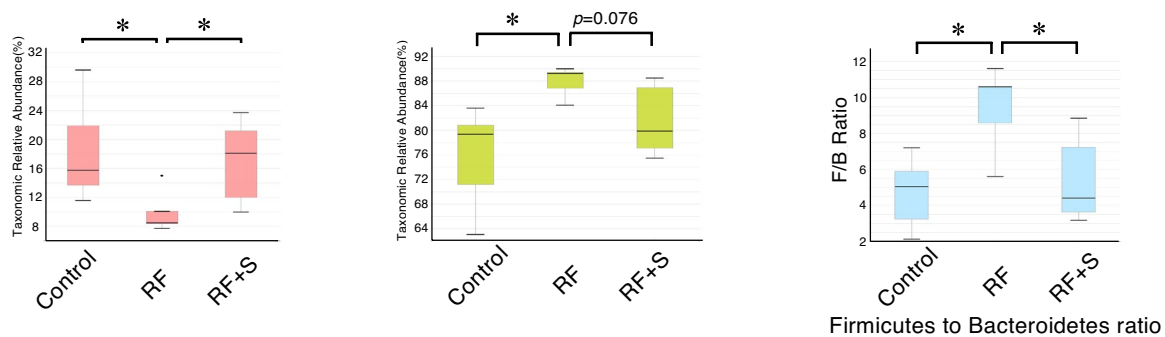
(c) Unweighted UniFrac PCoA



Weighted UniFrac PCoA



(e)



phylum

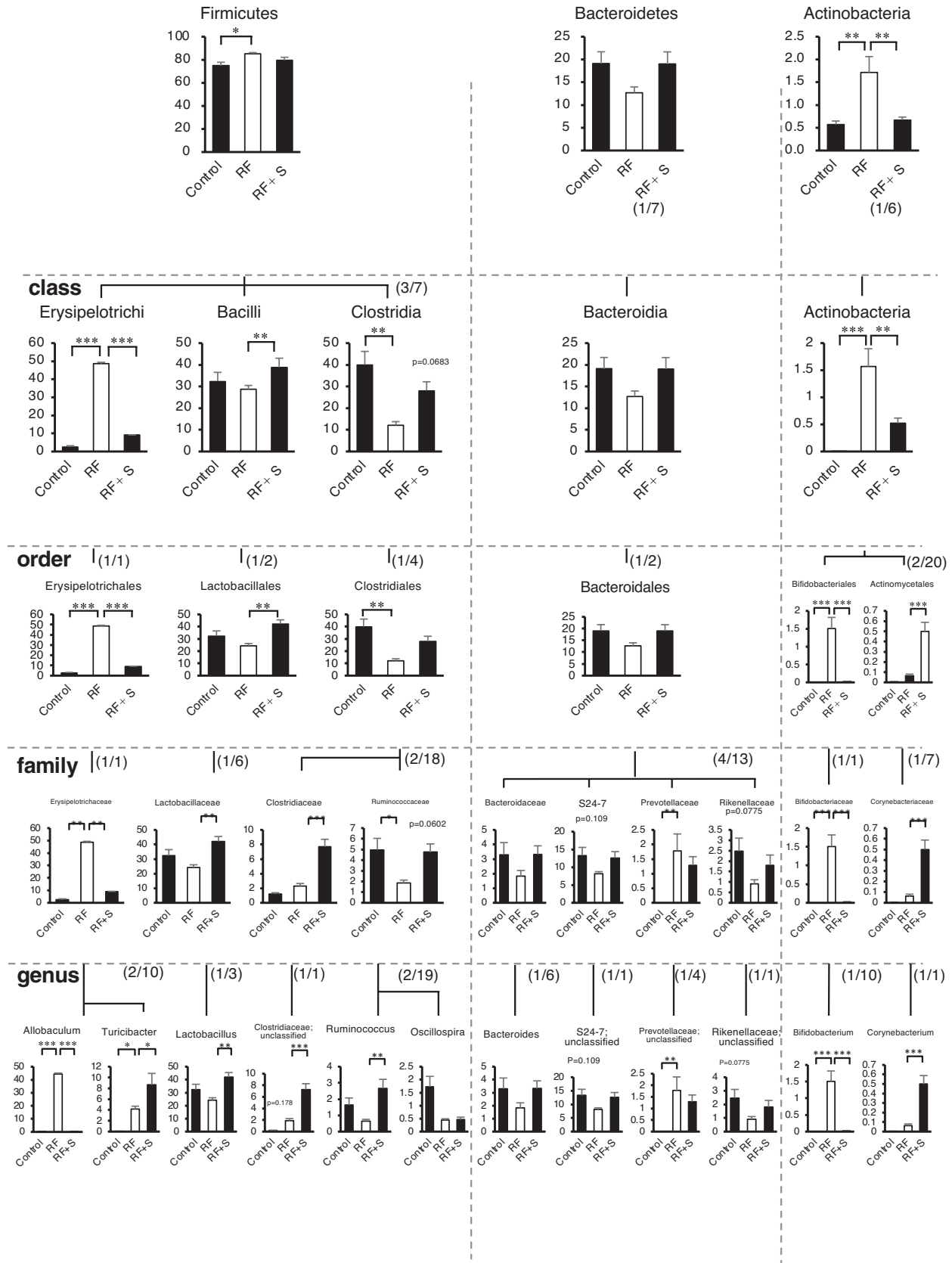


FIGURE 6 Relative abundance of microbiota based on the average abundance of each subgroup at order, family, and genus levels. Statistical analysis was performed using a Dunnett's test. * $p < 0.05$ and ** $p < 0.01$ were treated as statistically significant. Cont: control group, RF: renal failure group; RF + SGL5213 ($n = 8$ for each group)

3.5 | SGL5213 partially inhibit tyrosine phenol-lyase activity

DKD is a major cause of RF and is in urgent need of a breakthrough in disease management (Pavkov et al., 2012). We reported that PS is a marker and modifiable therapeutic target for DKD patients (Kikuchi et al., 2019). Dietary L-tyrosine is converted into phenol in the gut by gut bacterial-specific TPL (EC 4.1.99.2) (Watkins & Phillips, 2001), and absorbed phenol is metabolized into PS in the liver (Kikuchi et al., 2019). The TPL-specific inhibitors 2-aza-tyrosine (Watkins & Phillips, 2001) and L-meta-tyrosine (Bertin et al., 2007) reduced plasma PS levels (Kikuchi et al., 2019). In addition, it has been reported that the estimated drug concentrations in the small intestine and colon are higher than the plasma concentration (Maier et al., 2018), and susceptibility to human-targeted drugs correlates across bacterial species with anti-commensal activity. Because SGL5213 reduced the PS level in the RF model, we measured the concentration of SGL5213 in the feces. The concentration of SGL5213 in the feces varied from 11.9 to 202 nmol/g (~93.3 μ M)

(Figure 7a). To further clarify the effect of reducing PS, we examined the effect of SGL5213 on gut microbial-derived TPL enzyme activity. One mM of the specific TPL inhibitor 2-aza-tyrosine (Watkins & Phillips, 2001), SGL5213, and SGL2/1 inhibitor canagliflozin significantly and comparably inhibited TPL activity (Figure 7b). At 300 μ M, 2-aza-tyrosine was still completely inhibited, but neither SGL5213 nor canagliflozin inhibited TPL activity. These data suggest that the changes in microbiota may be “secondary” to improvement in host homeostasis and reduced uremic toxins.

4 | DISCUSSION

SGLT2 is predominantly located in the kidney and is responsible for 90% glucose reabsorption in the kidney (Wright et al., 2011), whereas SGLT1 is mainly located in the brush border membrane of the small intestine and plays a critical role in glucose absorption (Gorboulev et al., 2012). These results indicate the renal absorption contribution rate of SGLT1 (10%) and SGLT2 (90%) in the

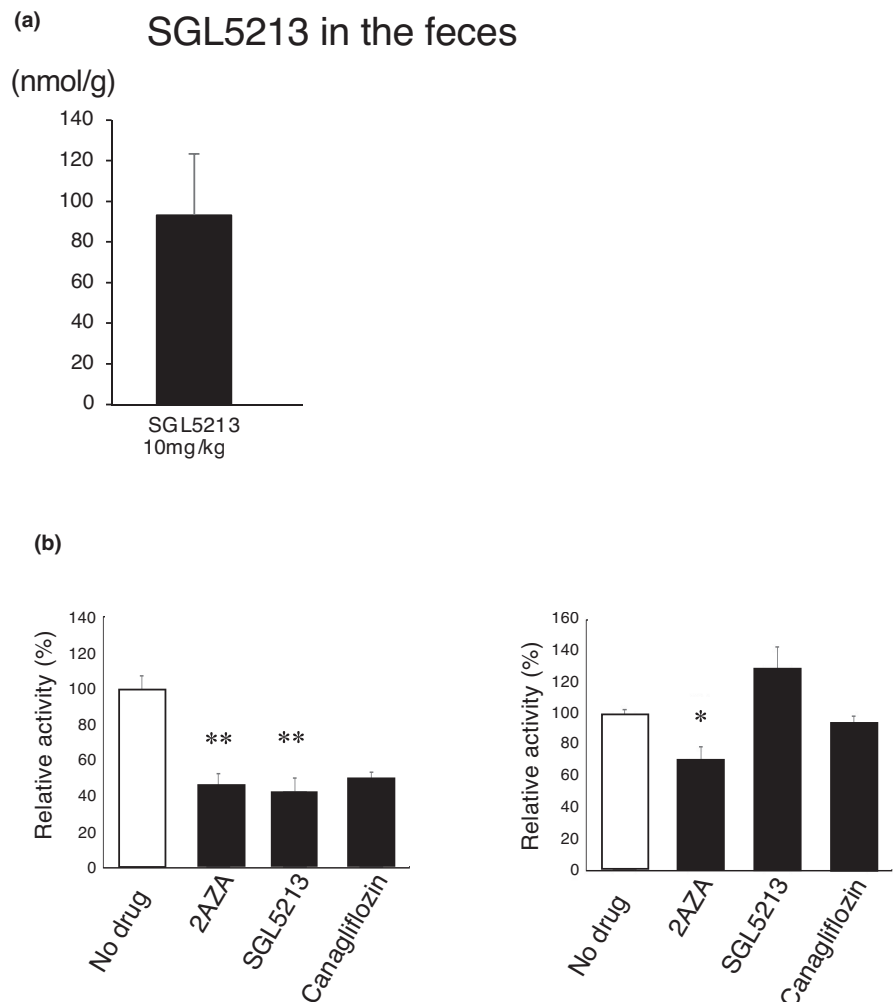


FIGURE 7 Concentration of SGL5213 in the feces and effect on TPL activity. (a) The concentration of SGL5213 in the feces was measured by LC/MS/MS. Cont: control group ($n = 8$); RF; renal failure group ($n = 6$); RF treated with SGL5213 (10 mg/kg/day) group ($n = 8-9$ each). Data were mean \pm SEM. (b) Effect of SGL5213 on TPL activity. One millimolar of the specific TPL inhibitor 2-aza-tyrosine, SGL5213, and canagliflozin (SGLT2/1 inhibitor) significantly and comparably inhibited the TPL activity. At 300 μ M, 2-aza-tyrosine (2-AZA) still completely and SGL5213 partly inhibited TPL activity. Data were mean \pm SEM. Statistical analyses were performed using a Dunnett's test. * $p < 0.05$ was treated as statistically significant

kidney (Wright et al., 2011). SGLT1 is the primary transporter for glucose absorption from digested nutrients in the gastrointestinal tract (Io et al., 2019). SGLT1-mediated glucose translocation across the BBM is a rate-limiting step in small intestinal glucose absorption (Gorboulev et al., 2012; Koepsell, 2017). A reduction in glucose absorption in the duodenum and jejunum changes the glucose concentrations in the ileum and colon, which may influence the secretion of gastrointestinal hormones as well as the gut microbiota (Koepsell, 2017). Recently, we reported that canagliflozin, a dual SGLT1/2 inhibitor, reduced the plasma levels of IS and PCS by influencing the intestinal environment in mice with adenine-induced RF, such as bacterial carbohydrate fermentation (Mishima et al., 2018). Accordingly, we further examined the gut-specific effect of SGLT1 inhibitor SGL5213, which inhibits SGLT1 in the small intestine. We found that SGL5213 ameliorated renal damage and dysfunction by modifying the gut microbiota community.

Concerning the renoprotective effect of SGL5213, two possible causes are suggested: First, our study revealed that SGL5213 inhibited intestinal glucose absorption and that excess glucose might enhance bacterial carbohydrate fermentation, thereby ameliorating the intestinal microbiota composition in RF mice. We also measured the intestinal and fecal glucose levels (Figure 2a). Although the secretion of glucose into the intestinal fluid was significantly increased in the RF + SGL5213 group compared with the RF group, the fecal glucose level did not change, suggesting that the transit glucose is used in the gut. Indeed, it was anticipated that SGL5213 would reduce the accumulation of gut-derived uremic toxins by modifying the gut microbiota, which could delay the onset of RF, providing a novel and potential therapeutic tool for CKD patients. Second, colonic transit time is a highly important factor to consider in microbiome and metabolomic studies (Roager et al., 2016). We and other groups reported that several laxatives, lubiprostone (Mishima et al., 2015), linaclotide (Nanto-Hara et al., 2020), and lactulose (Sueyoshi et al., 2019) modify the gut microbiota and ameliorate CKD progression by suppressing uremic toxin production. Genetic mutations within the SGLT1 gene (*Slc5a1*) in humans are associated with the neonatal onset of severe life-threatening diarrhea and dehydration due to increased colonic carbohydrates (Al-Lawama et al., 2019; Lehmann & Hornby, 2016). Oral administration of an SGLT1 selective inhibitor in diabetic rat models also reduced blood glucose, with diarrhea occurring even at a higher dose (Fushimi et al., 2013). In this study, the weight of feces did not change and no obvious diarrhea was observed, suggesting that the renoprotective effect of SGL5213 is not dependent on decreasing colonic transit (Roager et al., 2016).

SGL5213 also reduced the uric acid allantoin levels. Because allantoin is a urate oxidation product (Becker, 1993) and these compounds may increase as a result of the oxidative state in RF, SGL5213 also reduced the renoprotective effect by reducing oxidative stress.

We also found that SGL5213 modulated the gut microbiota composition, characterized by a decreased ratio of Firmicutes to Bacteroidetes and reduced abundance of *Allobaculum* in RF mice. *Allobaculum* is an important functional phylotype of metabolic dysbiosis (Nobel et al., 2015) (Jia et al., 2017). In response to a high-fat diet (HFD), the B/F proportions reversed and the genus *Allobaculum*, known to be associated with HFD, increased (Nobel et al., 2015). Reduction of *Allobaculum* by SGL5213 can reverse the dysbiotic community. These data suggest that a change in the gut microbial ecosystem by SGL5213 could be an important factor to consider in microbiome and metabolomics studies.

In this study, we found that the F/B ratio in the RF was opposite to that in our previous study (Mishima et al., 2018). It is widely recognized that the intestinal microbiota plays an essential role in health and disease. However, mice bred in the same facility or purchased from a vendor sometimes display differences in the intestinal microbial community (Franklin & Ericsson, 2017). It has also been reported that microbiota differs between commercial breeders and company sourced mice. Diet and other important considerations may determine the model reproducibility (Ericsson & Franklin, 2021) and phenotype (Sadler et al., 2017). Therefore, we tried to obtain mice from the same supplier that produced commercially available laboratory mice and carefully interpreted the results.

Among gut-derived uremic toxins, SGL5213 significantly decreased the PS (Figure 3d). PS is a metabolite of phenol in humans and is synthesized from dietary L-tyrosine by gut bacterial TPL (Watkins & Phillips, 2001). TPL inhibition decreases plasma PS levels without inducing host toxicity (Kikuchi et al., 2019). We recently reported that a reduction in PS is a potent therapeutic target for diabetic nephropathy (Kikuchi et al., 2019). Here, we report that SGL5213 reduced the plasma PS level as well as that of glucose, and therefore, could be an ideal drug for diabetic nephropathy. TPL inhibition reduces albuminuria in diabetic mice (Kikuchi et al., 2019). Because it is well known that the estimated drug concentrations in the small intestine and colon are higher than the plasma concentration (Maier et al., 2018), we measured the SGL5213 concentration in the feces. Our data suggest that the effect of SGT15213 on PS reduction may depend mainly on changes in the gut microbiome community. Recently, it was reported that susceptibility to antibiotics and human-targeted drugs correlates across bacterial species with anti-commensal

activity. A high concentration of SGLL5213 in feces may result, in part, to a reduction in PS.

Here, we used adenine-induced CKD mice that crystallized adenine accumulated within the nephron, and the damage was reversible after stopping feeding (Kamijio-Ikemori et al., 2016; Mishima et al., 2015). To clarify the characteristics of diabetic DKD with Kimmelstiel–Wilson nodules (Conti et al., 2018; Thomas et al., 2015). In mice, there are few models that are suitable for exploring DKD as KK-Ay/Ta (Ito et al., 2006) or mice lacking eNOS by introducing the Akita mutation in the insulin2 gene (Kikuchi et al., 2019). In addition, the experiment should be longer in length, if possible, extending several months. Furthermore, different long-span experiments are needed to determine the effect of SGL5213 on DKD.

In conclusion, SGL5213 is an ideal candidate for DKD that promotes the reduction of blood glucose and gut-derived uremic toxins (especially PS), as well as controlling the bacterial commensal community.

ACKNOWLEDGMENTS

The authors thank Fumiko Date, Miki Yoshizawa, and Naoko Shibata (Histological platform, Tohoku University School of Medicine) for their histological assistance.

CONFLICT OF INTEREST

None.

AUTHOR CONTRIBUTIONS

Conceptualization: Hsin-Jung Ho, Takaaki Abe. Data curation: Yoshitomi Kanemitsu, Daisuke Saigusa. Formal analysis: Hsin-Jung Ho. Funding acquisition: Takaaki Abe. Investigation: Hsin-Jung Ho, Koichi Kikuchi, Daiki Oikawa, Shun Watanabe, Yoshitomi Kanemitsu, Ryota Kujirai, Wakako Ohtsubo, Mariko Ichijo, and Yukako Akiyama. As well as Eikan Mishima, Yoshiaki Ogata, Yoshitsugu Oikawa, Tetsuro Matsushashi, Takafumi Toyohara, Chitose Suzuki, Takehiro Suzuki, and Takane Katayama. Statistical analysis: Hsin-Jung Ho, Koichi Kikuchi, and Yuichi Aoki. Project administration: Takaaki Abe. Histological analysis: Yoshiteru Kagawa, Yuji Owada. Tyrosine measurement: Ryota Kujirai. Supervision: Toru Nakayama, Nariyasu Mano, Yoshihisa Tomioka, and Takaaki Abe. Writing—original draft: Hsin-Jung Ho, Takaaki Abe. Writing—review and editing: Hsin-Jung Ho, Koichi Kikuchi, Takaaki Abe.

ORCID

Takaaki Abe  <https://orcid.org/0000-0003-3170-4660>

REFERENCES

Alicic, R. Z., Neumiller, J. J., Johnson, E. J., Dieter, B., & Tuttle, K. R. (2019). Sodium-glucose cotransporter 2 inhibition and diabetic

kidney disease. *Diabetes*, 68, 248–257. <https://doi.org/10.2337/dbi18-0007>.

- Al-Lawama, M., Albaramki, J., Altamimi, M., & El-Shanti, H. (2019). Congenital glucose-galactose malabsorption: A case report with a novel SLC5A1 mutation. *Clinical Case Reports*, 7, 51–53.
- Balis, D. A., Tong, C., & Meininger, G. (2014). Effect of canagliflozin, a sodium-glucose cotransporter 2 inhibitor, on measurement of serum 1,5-anhydroglucitol. *Journal of Diabetes*, 6, 378–380.
- Becker, B. F. (1993). Towards the physiological function of uric acid. *Free Radical Biology and Medicine*, 14, 615–631. [https://doi.org/10.1016/0891-5849\(93\)90143-I](https://doi.org/10.1016/0891-5849(93)90143-I).
- Bertin, C., Weston, L. A., Huang, T., Jander, G., Owens, T., Meinwald, J., & Schroeder, F. C. (2007). Grass roots chemistry: meta-tyrosine, an herbicidal nonprotein amino acid. *Proceedings of the National Academy of Sciences of the United States of America*, 104, 16964–16969.
- Biasioli, S., Feriani, M., Bigi, L., Dell'Aquila, R., Bragantini, L., Chiaramonte, S., Fabris, A., Brendolan, A., Ronco, C., Pradella, M., Cesaro, A., & La Greca, G. (1987). Tricarboxylic acid cycle intermediates in chronic renal failure. *Nephrology, Dialysis, Transplantation*, 2, 313–315.
- Caporaso, J. G., Kuczynski, J., Stombaugh, J., Bittinger, K., Bushman, F. D., Costello, E. K., Fierer, N., Pena, A. G., Goodrich, J. K., Gordon, J. I., Huttley, G. A., Kelley, S. T., Knights, D., Koenig, J. E., Ley, R. E., Lozupone, C. A., McDonald, D., Muegge, B. D., Pirrung, M., ... Knight, R. (2010). QIIME allows analysis of high-throughput community sequencing data. *Nature Methods*, 7, 335–336. <https://doi.org/10.1038/nmeth.f.303>.
- Conti, S., Perico, N., Novelli, R., Carrara, C., Benigni, A., & Remuzzi, G. (2018). Early and late scanning electron microscopy findings in diabetic kidney disease. *Scientific Reports*, 8, 4909.
- Ericsson, A. C., & Franklin, C. L. (2021). The gut microbiome of laboratory mice: considerations and best practices for translational research. *Mammalian Genome*. <https://doi.org/10.1007/s00335-021-09863-7>.
- Franklin, C. L., & Ericsson, A. C. (2017). Microbiota and reproducibility of rodent models. *Lab Animal*, 46, 114–122. <https://doi.org/10.1038/labana.1222>.
- Fushimi, N., Teranishi, H., Shimizu, K., Yonekubo, S., Ohno, K., Miyagi, T., Itoh, F., Shibazaki, T., Tomae, M., Ishikawa-Takemura, Y., Nakabayashi, T., Kamada, N., Yamauchi, Y., Kobayashi, S., & Isaji, M. (2013). Design, synthesis, and structure-activity relationships of a series of 4-benzyl-5-isopropyl-1H-pyrazol-3-yl beta-D-glycopyranosides substituted with novel hydrophilic groups as highly potent inhibitors of sodium glucose co-transporter 1 (SGLT1). *Bioorganic & Medicinal Chemistry*, 21, 748–765.
- Gorboulev, V., Schurmann, A., Vallon, V., Kipp, H., Jaschke, A., Klessen, D., Friedrich, A., Scherneck, S., Rieg, T., Cunard, R., Veyhl-Wichmann, M., Srinivasan, A., Balen, D., Breljak, D., Rexhepaj, R., Parker, H. E., Gribble, F. M., Reimann, F., Lang, F., ... Koepsell, H. (2012). Na(+)-D-glucose cotransporter SGLT1 is pivotal for intestinal glucose absorption and glucose-dependent incretin secretion. *Diabetes*, 61, 187–196. <https://doi.org/10.2337/db11-1029>.
- Io, F., Gunji, E., Koretsune, H., Kato, K., Sugisaki-Kitano, M., Okumura-Kitajima, L., Kimura, K., Uchida, S., & Yamamoto, K. (2019). SGL5213, a novel and potent intestinal SGLT1 inhibitor, suppresses intestinal glucose absorption and enhances plasma GLP-1 and GLP-2 secretion in rats. *European Journal*

- of *Pharmacology*, 853, 136–144. <https://doi.org/10.1016/j.ejphar.2019.03.023>.
- Ito, T., Tanimoto, M., Yamada, K., Kaneko, S., Matsumoto, M., Obayashi, K., Hagiwara, S., Murakoshi, M., Aoki, T., Wakabayashi, M., Gohda, T., Funabiki, K., Maeda, K., Horikoshi, S., & Tomino, Y. (2006). Glomerular changes in the KK-Ay/Ta mouse: a possible model for human type 2 diabetic nephropathy. *Nephrology (Carlton)*, 11, 29–35.
- Jha, V., Garcia-Garcia, G., Iseki, K., Li, Z., Naicker, S., Plattner, B., Saran, R., Wang, A. Y., & Yang, C. W. (2013). Chronic kidney disease: Global dimension and perspectives. *Lancet*, 382, 260–272.
- Jia, L., Li, D., Feng, N., Shamon, M., Sun, Z., Ding, L., Zhang, H., Chen, W., Sun, J., & Chen, Y. Q. (2017). Anti-diabetic effects of clostridium butyricum CGMCC0313.1 through promoting the growth of gut butyrate-producing bacteria in type 2 diabetic mice. *Scientific Reports*, 7, 7046. <https://doi.org/10.1038/s41598-017-07335-0>.
- Kalra, S., Singh, V., & Nagrale, D. (2016). Sodium-glucose cotransporter-2 inhibition and the glomerulus: A review. *Advances in Therapy*, 33, 1502–1518.
- Kamijo-Ikemori, A., Sugaya, T., Hibi, C., Nakamura, T., Murase, T., Oikawa, T., Hoshino, S., Hisamichi, M., Hirata, K., Kimura, K., & Shibagaki, Y. (2016). Renoprotective effect of the xanthine oxidoreductase inhibitor topiroxostat on adenine-induced renal injury. *American Journal of Physiology Renal Physiology*, 310, F1366–1376. <https://doi.org/10.1152/ajprenal.00517.2015>.
- Kand'ar, R., & Zakova, P. (2008). Allantoin as a marker of oxidative stress in human erythrocytes. *Clinical Chemistry and Laboratory Medicine*, 46, 1270–1274. <https://doi.org/10.1515/CCLM.2008.244>.
- Kanemitsu, Y., Asaji, K., Matsumoto, Y., Tsukamoto, H., Saigusa, D., Mukawa, C., Tachikawa, T., Abe, T., & Tomioka, Y. (2017). Simultaneous quantitative analysis of uremic toxins by LC-MS/MS with a reversed-phase/cation-exchange/anion-exchange tri-modal mixed-mode column. *Journal of Chromatography B, Analytical Technologies in the Biomedical and Life Sciences*, 1068–1069, 1–8. <https://doi.org/10.1016/j.jchromb.2017.10.009>.
- Katayama, T., Suzuki, H., Koyanagi, T., & Kumagai, H. (2000). Cloning and random mutagenesis of the *Erwinia herbicola* tyrR gene for high-level expression of tyrosine phenol-lyase. *Applied and Environment Microbiology*, 66, 4764–4771.
- Kikuchi, K., Saigusa, D., Kanemitsu, Y., Matsumoto, Y., Thanai, P., Suzuki, N., Mise, K., Yamaguchi, H., Nakamura, T., Asaji, K., Mukawa, C., Tsukamoto, H., Sato, T., Oikawa, Y., Iwasaki, T., Oe, Y., Tsukimi, T., Fukuda, N. N., Ho, H. J., ... Abe, T. (2019). Gut microbiome-derived phenyl sulfate contributes to albuminuria in diabetic kidney disease. *Nature Communications*, 10, 1835. <https://doi.org/10.1038/s41467-019-09735-4>.
- Koepsell, H. (2017). The Na(+)-D-glucose cotransporters SGLT1 and SGLT2 are targets for the treatment of diabetes and cancer. *Pharmacology & Therapeutics*, 170, 148–165. <https://doi.org/10.1016/j.pharmthera.2016.10.017>.
- Kuroda, S., Kobashi, Y., Oi, T., Amada, H., Okumura-Kitajima, L., Io, F., Yamamoto, K., & Kakinuma, H. (2018). Discovery of a potent, low-absorbable sodium-dependent glucose cotransporter 1 (SGLT1) inhibitor (TP0438836) for the treatment of type 2 diabetes. *Bioorganic & Medicinal Chemistry Letters*, 28, 3534–3539. <https://doi.org/10.1016/j.bmcl.2018.09.035>.
- Kuroda, S., Kobashi, Y., Oi, T., Kawabe, K., Shiozawa, F., Okumura-Kitajima, L., Sugisaki-Kitano, M., Io, F., Yamamoto, K., & Kakinuma, H. (2019). Discovery of potent, low-absorbable sodium-dependent glucose cotransporter 1 (SGLT1) inhibitor SGL5213 for type 2 diabetes treatment. *Bioorganic & Medicinal Chemistry*, 27, 394–409. <https://doi.org/10.1016/j.bmc.2018.12.015>.
- Lehmann, A., & Hornby, P. J. (2016). Intestinal SGLT1 in metabolic health and disease. *American Journal of Physiology Gastrointestinal and Liver Physiology*, 310, G887–898. <https://doi.org/10.1152/ajpgi.00068.2016>.
- Maier, L., Pruteanu, M., Kuhn, M., Zeller, G., Telzerow, A., Anderson, E. E., Brochado, A. R., Fernandez, K. C., Dose, H., Mori, H., Patil, K. R., Bork, P., & Typas, A. (2018). Extensive impact of non-antibiotic drugs on human gut bacteria. *Nature*, 555, 623–628. <https://doi.org/10.1038/nature25979>.
- Mishima, E., Fukuda, S., Kanemitsu, Y., Saigusa, D., Mukawa, C., Asaji, K., Matsumoto, Y., Tsukamoto, H., Tachikawa, T., Tsukimi, T., Fukuda, N. N., Ho, H. J., Kikuchi, K., Suzuki, C., Nanto, F., Suzuki, T., Ito, S., Soga, T., Tomioka, Y., & Abe, T. (2018). Canagliflozin reduces plasma uremic toxins and alters the intestinal microbiota composition in a chronic kidney disease mouse model. *American Journal of Physiology-Renal Physiology*, 315(4), F824–F833. <https://doi.org/10.1152/ajprenal.00314.2017>.
- Mishima, E., Fukuda, S., Mukawa, C., Yuri, A., Kanemitsu, Y., Matsumoto, Y., Akiyama, Y., Fukuda, N. N., Tsukamoto, H., Asaji, K., Shima, H., Kikuchi, K., Suzuki, C., Suzuki, T., Tomioka, Y., Soga, T., Ito, S., & Abe, T. (2017). Evaluation of the impact of gut microbiota on uremic solute accumulation by a CE-TOFMS-based metabolomics approach. *Kidney International*, 92, 634–645. <https://doi.org/10.1016/j.kint.2017.02.011>.
- Mishima, E., Fukuda, S., Shima, H., Hirayama, A., Akiyama, Y., Takeuchi, Y., Fukuda, N. N., Suzuki, T., Suzuki, C., Yuri, A., Kikuchi, K., Tomioka, Y., Ito, S., Soga, T., & Abe, T. (2015). Alteration of the intestinal environment by lubiprostone is associated with amelioration of adenine-induced CKD. *Journal of the American Society of Nephrology*, 26, 1787–1794. <https://doi.org/10.1681/ASN.2014060530>.
- Murakami, S., Goto, Y., Ito, K., Hayasaka, S., Kurihara, S., Soga, T., Tomita, M., & Fukuda, S. (2015). The consumption of bicarbonate-rich mineral water improves glycemic control. *Evidence-Based Complementary and Alternative Medicine: Ecam*, 2015, 824395. <https://doi.org/10.1155/2015/824395>.
- Nanto-Hara, F., Kanemitsu, Y., Fukuda, S., Kikuchi, K., Asaji, K., Saigusa, D., Iwasaki, T., Ho, H. J., Mishima, E., Suzuki, T., Suzuki, C., Tsukimi, T., Matsuhashi, T., Oikawa, Y., Akiyama, Y., Kure, S., Owada, Y., Tomioka, Y., Soga, T., ... Abe, T. (2020). The guanlylate cyclase C agonist linaclotide ameliorates the gut-cardio-renal axis in an adenine-induced mouse model of chronic kidney disease. *Nephrology, Dialysis, Transplantation*, 35, 250–264. <https://doi.org/10.1093/ndt/gfz126>.
- Nobel, Y. R., Cox, L. M., Kirigin, F. F., Bokulich, N. A., Yamanishi, S., Teitler, I., Chung, J., Sohn, J., Barber, C. M., Goldfarb, D. S., Raju, K., Abubucker, S., Zhou, Y., Ruiz, V. E., Li, H., Mitreva, M., Alekseyenko, A. V., Weinstock, G. M., Sodergren, E., & Blaser, M. J. (2015). Metabolic and metagenomic outcomes from early-life pulsed antibiotic treatment. *Nature Communications*, 6, 7486. <https://doi.org/10.1038/ncomms8486>.

- Oguma, T., Nakayama, K., Kuriyama, C., Matsushita, Y., Yoshida, K., Hikida, K., Obokata, N., Tsuda-Tsukimoto, M., Saito, A., Arakawa, K., Ueta, K., & Shiotani, M. (2015). Intestinal sodium glucose cotransporter 1 inhibition enhances glucagon-like peptide-1 secretion in normal and diabetic rodents. *Journal of Pharmacology and Experimental Therapeutics*, *354*, 279–289. <https://doi.org/10.1124/jpet.115.225508>.
- Pavkov, M. E., Knowler, W. C., Lemley, K. V., Mason, C. C., Myers, B. D., & Nelson, R. G. (2012). Early renal function decline in type 2 diabetes. *Clinical Journal of the American Society of Nephrology*, *7*, 78–84. <https://doi.org/10.2215/CJN.07610711>.
- Perkovic, V., de Zeeuw, D., Mahaffey, K. W., Fulcher, G., Erond, N., Shaw, W., Barrett, T. D., Weidner-Wells, M., Deng, H., Matthews, D. R., & Neal, B. (2018). Canagliflozin and renal outcomes in type 2 diabetes: Results from the CANVAS program randomised clinical trials. *The Lancet Diabetes & Endocrinology*, *6*, 691–704.
- Phillips, R. S. (1987). Reactions of O-acyl-L-serines with tryptophanase, tyrosine phenol-lyase, and tryptophan synthase. *Archives of Biochemistry and Biophysics*, *256*, 302–310. [https://doi.org/10.1016/0003-9861\(87\)90450-4](https://doi.org/10.1016/0003-9861(87)90450-4).
- Phillips, R., Ravichandran, K., & Von Tersch, R. (1989). Synthesis of L-tyrosine from phenol and S-(o-nitrophenyl)-cysteine catalysed by tyrosine phenol-lyase. *Enzyme and Microbial Technology*, *11*, 80–83.
- Ritz, E., & Orth, S. R. (1999). Nephropathy in patients with type 2 diabetes mellitus. *The New England Journal of Medicine*, *341*, 1127–1133. <https://doi.org/10.1056/NEJM199910073411506>.
- Roager, H. M., Hansen, L. B., Bahl, M. I., Frandsen, H. L., Carvalho, V., Gobel, R. J., Dalgaard, M. D., Plichta, D. R., Sparholt, M. H., Vestergaard, H., Hansen, T., Sicheritz-Ponten, T., Nielsen, H. B., Pedersen, O., Lauritzen, L., Kristensen, M., Gupta, R., & Licht, T. R. (2016). Colonic transit time is related to bacterial metabolism and mucosal turnover in the gut. *Nature Microbiology*, *1*, 16093. <https://doi.org/10.1038/nmicrobiol.2016.93>.
- Roder, P. V., Geillinger, K. E., Zietek, T. S., Thorens, B., Koepsell, H., & Daniel, H. (2014). The role of SGLT1 and GLUT2 in intestinal glucose transport and sensing. *PLoS One*, *9*, e89977. <https://doi.org/10.1371/journal.pone.0089977>.
- Sadler, R., Singh, V., Benakis, C., Garzetti, D., Brea, D., Stecher, B., Anrather, J., & Liesz, A. (2017). Microbiota differences between commercial breeders impacts the post-stroke immune response. *Brain, Behavior, and Immunity*, *66*, 23–30. <https://doi.org/10.1016/j.bbi.2017.03.011>.
- Sueyoshi, M., Fukunaga, M., Mei, M., Nakajima, A., Tanaka, G., Murase, T., Narita, Y., Hirata, S., & Kadowaki, D. (2019). Effects of lactulose on renal function and gut microbiota in adenine-induced chronic kidney disease rats. *Clinical and Experimental Nephrology*, *23*, 908–919. <https://doi.org/10.1007/s10157-019-01727-4>.
- Sundararaju, B., Antson, A. A., Phillips, R. S., Demidkina, T. V., Barbolina, M. V., Gollnick, P., Dodson, G. G., & Wilson, K. S. (1997). The crystal structure of Citrobacter freundii tyrosine phenol-lyase complexed with 3-(4'-hydroxyphenyl)propionic acid, together with site-directed mutagenesis and kinetic analysis, demonstrates that arginine 381 is required for substrate specificity. *Biochemistry*, *36*, 6502–6510.
- Thomas, M. C., Brownlee, M., Susztak, K., Sharma, K., Jandeleit-Dahm, K. A., Zoungas, S., Rossing, P., Groop, P. H., & Cooper, M. E. (2015). Diabetic kidney disease. *Nature Reviews Disease Primers*, *1*, 15018. <https://doi.org/10.1038/nrdp.2015.18>.
- Vaziri, N. D., Yuan, J., Nazertehrani, S., Ni, Z., & Liu, S. (2013). Chronic kidney disease causes disruption of gastric and small intestinal epithelial tight junction. *American Journal of Nephrology*, *38*, 99–103. <https://doi.org/10.1159/000353764>.
- Vaziri, N. D., Zhao, Y. Y., & Pahl, M. V. (2016). Altered intestinal microbial flora and impaired epithelial barrier structure and function in CKD: the nature, mechanisms, consequences and potential treatment. *Nephrology, Dialysis, Transplantation*, *31*, 737–746.
- Wanner, C., Inzucchi, S. E., Lachin, J. M., Fitchett, D., von Eynatten, M., Mattheus, M., Johansen, O. E., Woerle, H. J., Broedl, U. C., Zinman, B., & Investigators, E.-R.- O. (2016). Empagliflozin and progression of kidney disease in type 2 diabetes. *The New England Journal of Medicine*, *375*, 323–334. <https://doi.org/10.1056/NEJMoa1515920>.
- Watkins, E. B., & Phillips, R. S. (2001). Enzymatic synthesis of azal-tyrosines. *Bioorganic & Medicinal Chemistry Letters*, *11*, 2099–2100. [https://doi.org/10.1016/S0960-894X\(01\)00376-6](https://doi.org/10.1016/S0960-894X(01)00376-6).
- Weiner, D. E., Tighiouart, H., Amin, M. G., Stark, P. C., MacLeod, B., Griffith, J. L., Salem, D. N., Levey, A. S., & Sarnak, M. J. (2004). Chronic kidney disease as a risk factor for cardiovascular disease and all-cause mortality: A pooled analysis of community-based studies. *Journal of the American Society of Nephrology*, *15*, 1307–1315.
- Wright, E. M., Loo, D. D., & Hirayama, B. A. (2011). Biology of human sodium glucose transporters. *Physiological Reviews*, *91*, 733–794. <https://doi.org/10.1152/physrev.00055.2009>.
- Yang, T., Santisteban, M. M., Rodriguez, V., Li, E., Ahmari, N., Carvajal, J. M., Zadeh, M., Gong, M., Qi, Y., Zubcevic, J., Sahay, B., Pepine, C. J., Raizada, M. K., & Mohamadzadeh, M. (2015). Gut dysbiosis is linked to hypertension. *Hypertension*, *65*, 1331–1340. <https://doi.org/10.1161/HYPERTENSIONAHA.115.05315>.

SUPPORTING INFORMATION

Additional supporting information may be found in the online version of the article at the publisher's website.

How to cite this article: Ho, H.-J., Kikuchi, K., Oikawa, D., Watanabe, S., Kanemitsu, Y., Saigusa, D., Kujirai, R., Ikeda-Ohtsubo, W., Ichijo, M., Akiyama, Y., Aoki, Y., Mishima, E., Ogata, Y., Oikawa, Y., Matsushita, T., Toyohara, T., Suzuki, C., Suzuki, T., Mano, N., ... Abe, T. (2021). SGLT-1-specific inhibition ameliorates renal failure and alters the gut microbial community in mice with adenine-induced renal failure. *Physiological Reports*, *9*, e15092. <https://doi.org/10.14814/phy2.15092>